

#### INFRARED ABSORPTION SPECTRA OF ISOTOPICALLY-ENRICHED LITHIUM HYDRIDE

THESIS FOR THE DEGREE OF PH. D. MICHIGAN STATE UNIVERSITY

WALTER BRUCE ZIMMERMAN 1960



This is to certify that the

thesis entitled

INFRARED ABSORPTION SPECTRA

OF ISOTOPICALLY-ENRICHED LITHIUM HYDRIDE

presented by

Walter Bruce Zimmerman

has been accepted towards fulfillment of the requirements for

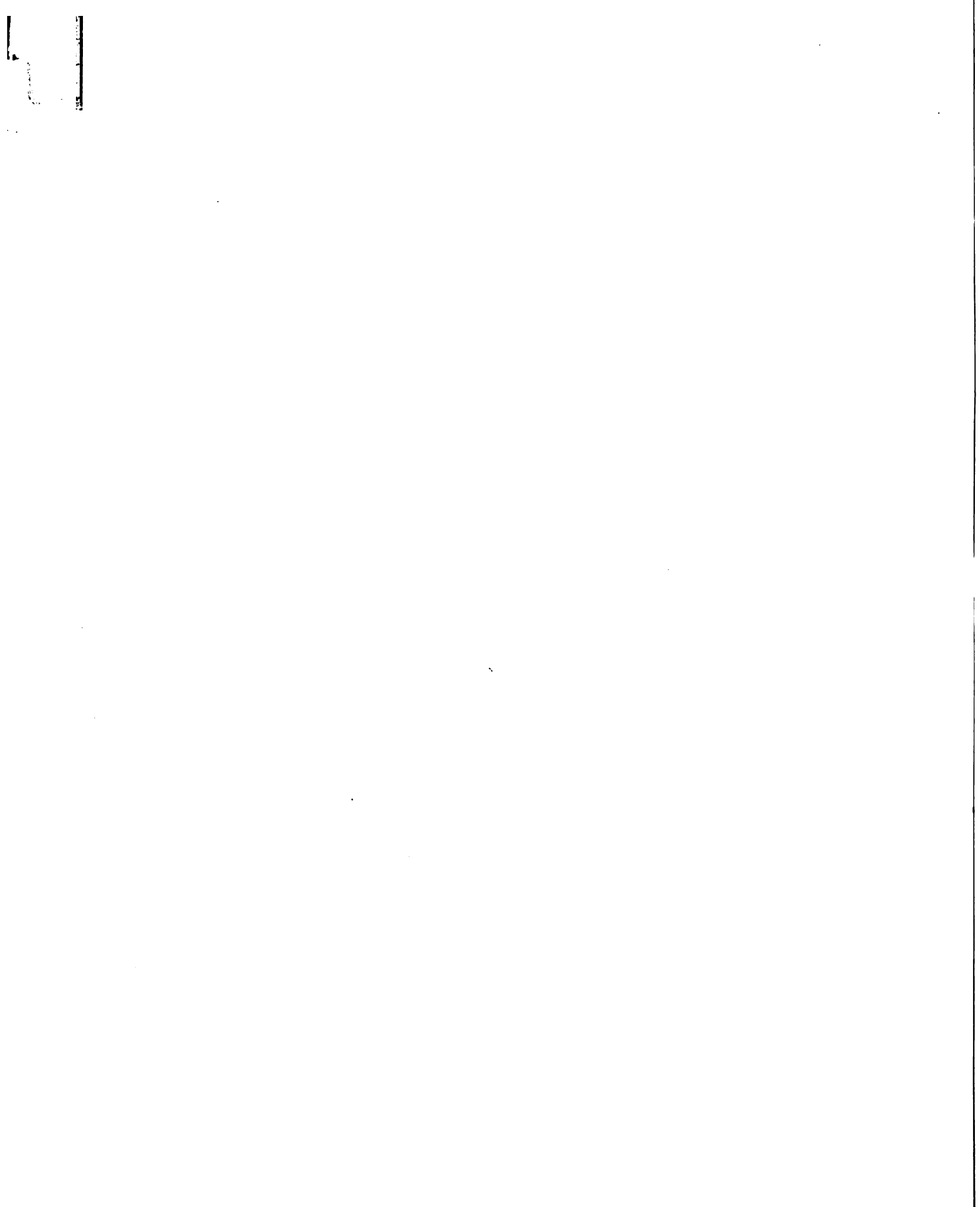
Ph.D. degree in Physics

Major professor

Date August 17, 1960

**O**-169





# INFRARED ABSORPTION SPECTRA OF ISOTOPICALLY-ENRICHED LITHIUM HYDRIDE

By

Walter Bruce Zimmerman

#### AN ABSTRACT

Submitted to the School for Advanced Graduate Studies of Michigan State University in partial fulfillment of the requirements for the degree of

DOCTOR OF PHILOSOPHY

Department of Physics and Astronomy

1960

Approved The report & Mayor

#### ABSTRACT

This work is an extension of a program exploiting isotopic mass and isotopic composition as probes for liquid-state and solid-state investigations to the study of the interaction of electromagnetic radiation with crystal lattices.

The infrared absorption spectrum of thin films (less than  $0.1\mu$ ) of solid lithium hydride made of varying proportions of its separated isotopes (Li<sup>6</sup>, Li<sup>7</sup>;H<sup>1</sup>, H<sup>2</sup>) was obtained at room temperature in the wavelength region of 12.5 to 25 $\mu$ . The primary feature of the spectrum of the relatively pure materials Li<sup>6</sup>H<sup>1</sup>, Li<sup>6</sup>H<sup>2</sup>, Li<sup>7</sup>H<sup>1</sup>, Li<sup>7</sup>H<sup>2</sup> is a broad but definite absorption peak at the dispersion wavelengths 16.9, 22.2, 17.0, 22.4  $\pm$  0.02 $\mu$ , respectively. The ratios of the dispersion wavelengths of Li<sup>6</sup>H<sup>2</sup> and Li<sup>6</sup>H<sup>1</sup>, Li<sup>7</sup>H<sup>2</sup> and Li<sup>6</sup>H<sup>2</sup> are: 1.31, 1.32, 1.01, 1.01  $\pm$  0.02, respectively, which are in excellent accord with the respective ratios of the square root of the reduced masses: 1.32, 1.33, 1.01,1.01. This agreement for the effect of isotopic mass on the dispersion wavelength of an ionic crystal is in accord with a prediction of the elementary Born theory of lattice vibrations.

The effect of isotopic composition on the infrared spectrum of mixtures of  $\text{Li}^6\text{H}^1$  and  $\text{Li}^6\text{H}^2$  appears to be complex. The dispersion wavelengths for the compositions  $\text{Li}^6[72.1\% \ \text{H}^1,\ 27.9\% \ \text{H}^2]$ ,  $\text{Li}^6[57.0\% \ \text{H}^1,\ 43.0\% \ \text{H}^2]$ ,  $\text{Li}^6[19.9\% \ \text{H}^1,\ 80.1\% \ \text{H}^2]$  are: 21.2, 21.4, 21.8  $\pm$  0.02 $\mu$ , respectively. The ratios of the dispersion wavelengths of  $\text{Li}^6[72.1\% \ \text{H}^1,\ 27.9\% \ \text{H}^2]$  and  $\text{Li}^6\text{H}^1$ ,  $\text{Li}^6[57.0\% \ \text{H}^1,\ 43.0\% \ \text{H}^2]$  and  $\text{Li}^6[72.1\% \ \text{H}^1,\ 27.9\% \ \text{H}^2]$ ,  $\text{Li}^6[19.9\% \ \text{H}^1,\ 80.1\% \ \text{H}^2]$  and  $\text{Li}^6[57.0\% \ \text{H}^1,\ 43.0\% \ \text{H}^2]$ ,  $\text{Li}^6\text{H}^2$  and  $\text{Li}^6[19.9\% \ \text{H}^1,\ 80.1\% \ \text{H}^2]$  are: 1.25, 1.01, 1.02, 1.02  $\pm$  0.02, respectively, which are in disagreement with the respective ratios of

the square roots of the average reduced masses: 1.09, 1.05, 1.10, 1.04. Therefore, the effect of isotopic composition on the dispersion wavelength of an ionic crystal cannot be explained simply by considering the composite film as being equivalent to one made up of isotopes with the average reduced mass.

## INFRARED ABSORPTION SPECTRA OF ISOTOPICALLY-ENRICHED LITHIUM HYDRIDE

By

Walter Bruce Zimmerman

#### A THESIS

Submitted to the School for Advanced Graduate Studies of Michigan State University in partial fulfillment of the requirements for the degree of

DOCTOR OF PHILOSOPHY

Department of Physics and Astronomy

G 20244 5/24/62

To Judy, Londa, and Devin

#### ACKNOWLEDGMENTS

The author wishes to thank Professor D. J. Montgomery for his suggestion of the problem and his instigation of the research. He would also like to express his sincere appreciation to him for his constant counsel and guidance.

The author gratefully recognizes and thanks:

Professor S. K. Haynes for assuming the Chairmanship of the Guidance Committee while Professor Montgomery is on sabbatical leave,

- Dr. N. T. Ban for his many suggestions and constructive criticism,
- Dr. T. H. Edwards for his suggestions on crystal polishing and metallizing,
- Dr. H. H. Eick of the Department of Chemistry for the use of a dry box and other equipment,
- Dr. P. S. Baker of the Stable Isotopes Research and Production Division of the Oak Ridge National Laboratory for supplying the samples of lithium-6 hydride and lithium-6 deuteride,
- Mr. J. B. Milgram of the Foote Mineral Company for supplying the lithium hydride sample,
- Mr. R. E. Miner of Metal Hydrides Incorporated for supplying the lithium deuteride sample,
- Mr. C. L. Kingston, Mr. N. Mercer and Mr. R. Hoskins for their fine work in the construction and renovation of the equipment,

The Atomic Energy Commission and the Air Force Office of Scientific Research for financial support, and

Many others who provided valuable help.

\*\*\*\*\*\*

#### TABLE OF CONTENTS

	Page
INTRODUCTION	. 1
A. Preliminary Considerations	
B. Choice of Material	. 2
C. Choice of Method	. 3
D. Statement of Problem	. 4
THEORY OF LONG OPTICAL VIBRATIONS AND INFRARE	D
DISPERSION	. 5
THEORY OF THE EXPERIMENT	. 14
APPARATUS AND METHOD	. 18
	. 10
A. Infrared Spectrophotometer	
B. Analysis of the Lithium Hydride Samples	
C. Film Preparation	
D. Measurement of Film Thickness	. 30
EXPERIMENTAL RESULTS	. 34
A. Effect of Isotopic Mass	. 35
B. Effect of Isotopic Composition	. 36
C. Measurement of Film Thickness	. 37
DISCUSSION OF RESULTS	. 41
A. Effect of Isotopic Mass	. 42
B. Effect of Isotopic Composition	. 43
C. Measurement of Film Thickness	. 44
REFERENCES CITED	. 45

### LIST OF FIGURES

Figure	Page
l. Infracord Block Diagram	19
2. Molybdenum Evaporating Boat	24
3. Sample Cell	26
4. Reference Cell	27
5. View of Experimental Setup	28
6. Method for Obtaining Fizeau Fringes	32
7. Fizeau Fringes from a Step 0.0691 μ Thick	33
8. Spectrum of Lithium Hydroxide Film	38
9. $I_0$ Spectrum with Cells in Respective Beams	38
10. Double Beam I <sub>0</sub>	38
11. Spectra of Lithium-6 or 7 in Combination with Hydrogen-1 or 2	39
12. Spectra of Composite Films	40

#### INTRODUCTION

## A. Preliminary Considerations\*

A valuable technique for investigating the behavior of matter in the aggregate is to vary the isotopic mass. Thus, in studying isotopes of the same element, the atomic mass can be changed while the atomic force field remains the same. Since the dependence on mass is usually simple, whereas the dependence on force field is very complicated, it is often feasible to make comparisons between isotopes of the same element when it is impractical to do so between different elements. A similar situation exists in compounds composed of elements whose isotopic mass can be changed. In the early days, however, the low enrichments obtainable precluded exploitation of isotopic mass in bulk studies. It was not until the establishment of atomic-energy projects that an array of elements became available in substantial amounts.

An example of this simple mass dependence occurs in the infrared dispersion frequency of ionic crystals which, according to elementary theory, varies inversely with the square root of the isotopic reduced mass. This dependence provides an interesting and important probe for the investigation of the interaction of electromagnetic radiation with crystal lattices. Knowledge of this interaction is important not only in analyzing the behavior of crystals, but also in the design of devices

<sup>\*</sup>Based on a paper by D. J. Montgomery, "Bulk Properties of Stable Isotopes as a Probe for Liquid-State and Solid-State Investigations," U. N. Peaceful Uses of Atomic Energy, Proc. Second Intern. Conf. 28, 165 (1958), and a research proposal to the Office of Naval Research by D. J. Montgomery, "Interaction of Electromagnetic Radiation with Crystal Lattices."

utilizing transmission, reflection, and absorption of radiation. Despite the attention paid to this field in recent years, there remain substantial regions of both the macroscopic and microscopic theory where the interpretation is inadequate or at least ambiguous. Specific examples are the value of the reflective power in the reflective band of the alkali halides; the existence of side bands near the main absorption or reflection bands in ionic crystals; the nature of the absorption bands in homopolar crystals; and the appearance of absorption irregularities at different wavelengths as observed by different investigators. In addition to phenomena not completely explained, numerous data are lacking: for example, the solid state infrared absorption spectra of the partially-ionic hydrides. Furthermore, almost no information exists on the effects of impurities, temperature, pressure, and isotopic composition.

No known experimental work exists on the problem of isotopic composition, and very little can be found in the literature on the theoretical aspect. Some introductory but unrealistic work has been done by Montroll and others<sup>1</sup> on one-dimensional lattices with isotopes at random, and Pirenne<sup>2</sup> has investigated the changes in the vibrational-frequency spectrum induced by isotopes. Unfortunately, the theory is not yet at the point where it can be compared with experimental results.

#### B. Choice of Material

The infrared absorption characteristics of many materials have been investigated. Among those with which little has been done is the interesting and important class of the hydrides. The common reason for neglecting this group of substances is the difficulty in handling them under normal conditions, for they are usually very hygroscopic. Experience gained in a program at Michigan State University on lithium and lithium fluoride suggested, however, that hydrides could be studied successfully if the effort were merited.

A number of advantages are afforded in the choice of lithium hydride. It may be obtained at reasonable cost in the form of lithium-6 or natural lithium depleted in lithium-6 in combination with natural hydrogen or deuterium. It is one of the few saline hydrides which melts and evaporates, thereby allowing preparation of thin films. More interesting yet are the large relative mass differences between hydrogen-1 and hydrogen-2 (67%) and between lithium-6 and lithium-7 (15%). Finally, it is one of the simplest of the partially-ionic materials with its atomic components of lithium and hydrogen having the low atomic numbers Z=3 and Z=1, respectively.

#### C. Choice of Method

Some of the more common methods used to prepare solid samples suitable for obtaining absorption spectra are: mulling, powder-film, mechanical-film, pressed-medium, melted-film, and evaporated-film.

The commonest and easiest method is the mulling technique in which the solid sample is mulled in a weakly-absorbing, non-volatile liquid. A part of the resultant paste is then spread over a substrate and placed in the sample beam of the spectrophotometer. However, sample thickness cannot be controlled accurately with this method.

In the powder-film technique, the powder is deposited directly as a film in the form of a residue upon evaporation of a liquid carrier.

This method is not popular because sample preparation is tedious.

A method which is applicable in a few cases is the mechanical-film technique in which sheets of suitable thickness can be obtained by use of a microtome or by scraping. Unfortunately, only a few materials lend themselves to this treatment.

The pressed-medium technique involves mixing the powdered sample in a finely-powdered medium without appreciable absorption in

the region of interest. The mixture is then inserted into a special die and subjected to heat and pressure under vacuum. A transparent disk is obtained, some of whose optical properties approach those of the original solid sample.

The melted-film technique has the advantage that the sample is never mixed with foreign materials (i.e., no mulling compounds or solutions are used), but thickness measurements are usually difficult.

With materials that evaporate, the evaporation technique has the same advantage of avoiding mixing of the sample with foreign materials. Furthermore, thickness measurements can be obtained relatively easily by optical means, and sample thickness can be controlled quite readily. Since lithium hydride does melt and evaporate, and because of the experience with evaporation earlier in the above-mentioned program at this university, the evaporated-film method was chosen.

#### D. Statement of Problem

It is proposed to obtain the infrared transmission spectra of isotopically-enriched lithium hydride in the form of thin films prepared by evaporation in the region from 12.5 $\mu$  to 25 $\mu$ . In particular, it is desired to obtain the infrared dispersion frequency (or wavelength) of such isotopically-enriched crystals, and to compare the experimental results with the predictions of current theory.

## THEORY OF LONG OPTICAL VIBRATIONS AND INFRARED DISPERSION<sup>3</sup>, <sup>5</sup>

It has been found that the optical lattice vibrations of large wavelengths (infrared) in an isotopically pure crystal can be considered on a macroscopic basis, i.e. whenever conditions are everywhere practically uniform over regions containing many lattice cells. Such optical vibrations are important chiefly in the ionic crystals because of the strong electric moments associated with the motion of the ions. For diatomic ionic crystals with optical isotropy, the macroscopic theory proves to be relatively simple, and the macroscopic description of the lattice motion can be embodied in a pair of equations called the lattice equations. In this discussion, these equations will be derived from an atomic standpoint, and the microscopic quantities will then be related to experimentally measurable macroscopic quantities.

A more complete theory is given in Chapter 7 of reference 3, and contains justification for some of the assumptions made in the elementary theory given below. However, because of the excessive computational work required by the more complete theory, no satisfactory theoretical results are as yet available for a quantitative comparison with experiment.

#### A. Derivation of the Lattice Equations

Consider a diatomic ionic crystal in an electric field E. Since the ionic and the electronic charges are displaced under the action of the electric field, special consideration must be given the long-range dipolar-interaction forces in contrast to the short-range forces due to chemical bonds, van der Waals attraction, and others. For the latter group of forces only the interaction between nearest neighbors need be considered, but for the former it is necessary to consider the entire atomic arrangement of the crystal.

To calculate the polarization P, one notes that the dipole moment is made up of two components: one due to the displacements of the ionic charges, and the other due to the induced electric moments of the ion. An ionic charge Ze displaced from its equilibrium position by a distance u is equivalent to a dipole of moment Zeu. But the induced electric moment p of an ion depends on the field acting upon the ion, and so it will be necessary to calculate the value of this field. This field will be called the effective field Eeff, and its value will be taken as that at the center of the ion.

The effective field Eeff is not the same as the macroscopic electric field E. The latter is the total field averaged over the space occupied by a lattice cell, while the former is the total field with the contribution of the ion itself excluded. It is clear that this difference is due only to the contributions to these fields of matter in the close neighborhood of the ion. Thus, a very good approximation can be made by neglecting those sources beyond a certain distance R in the calculation of the difference between the effective and macroscopic fields. Hence, let a sphere be drawn around the ion (which may be either positive or negative) with its radius R large compared to the lattice constant 0 so that the macroscopic quantities u, E, and P do not vary appreciably over it. The latter requirement is possible because 0 is a microscopic quantity in the present discussion.

The macroscopic field at the center of the sphere may easily be found by recalling that the polarization P of a homogeneous, isotropic medium is equivalent to a surface charge distribution with a density everywhere equal to the component of P along the outward normal to the surface. In the present case, it is evident from the symmetry that the field must have the same direction as P and so only contributions due to different surface elements in this direction need be considered. Introducing the

polar angles  $\theta$ ,  $\phi$  with the polar axis in the direction of  $\underline{P}$ , the field is calculated to be

$$\underline{E} = \int_0^{\pi} \int_0^{2\pi} (-\cos \theta) \frac{(\underline{P} \cos \theta)(\underline{R}^2 \sin \theta \ d \theta \ d \phi)}{\underline{R}^2} = -\frac{4\pi}{3} \underline{P}.$$

To calculate the effective field, the contribution of each ion to the field at the sphere center must be determined. Clearly, for the highly symmetrical crystals under consideration, the value of the field is zero when the ions are in their equilibrium positions, and so it is necessary only to calculate the field arising from the displaced and polarized ions. In view of the assumed uniformity of the macroscopic quantities over the spherical region, each of the ion sites may be considered to be occupied by a dipole equivalent to the sum of the displacement dipole Zeu and the induced dipole p. (The dipoles of each kind are identical with one another throughout the sphere.) The crux of the calculation is to note that the crystal symmetry is such that the crystal lattice is invariant under the tetrahedral group of operations, namely, rotations of  $\pi$  about the lattice axes and rotations of  $2\pi/3$  about the cube diagonals. Thus, Cartesian axes XYZ with their origin at the center of the sphere may be oriented in such manner that if there is an ion site with the coordinates (a, b, c), then there exist identical ion sites at the points (-a, -b, c), (a, -b, -c), (-a, b, -c), and eight additional points with coordinates obtained from the previous four by cyclic permutations of a, b, c. Then, by giving a, b, c appropriate values, sets of twelve points each are obtained which include all the ion sites in the sphere when taken together. For instance, a dipole  $p(p_1, p_2, p_3)$  at the point  $x_1(a, b, c)$ gives rise to a field at the origin of

$$-\frac{\underline{p}}{|\mathbf{x}_1|^3} + \frac{3\underline{p} \cdot \underline{x}_1}{|\mathbf{x}_2|^5} \underline{x}_1$$

Labeling the remaining eleven points by  $x_i$ , i=2,3,...,12, one calculates directly but tediously that the contribution to the effective field of the twelve identical dipoles is

$$-\frac{\sum_{i=1}^{12} \left[ \frac{p}{|\mathbf{x}_i|^3} - 3 \frac{\mathbf{p} \cdot \mathbf{x}_i}{|\mathbf{x}_i|^5} \frac{\mathbf{x}_i}{|\mathbf{x}_i|^5} \right]}{|\mathbf{x}_i|^5} = -\frac{\frac{12 p}{(a^2 + b^2 + c^2)^{\frac{3}{2}}}}{(a^2 + b^2 + c^2)^{\frac{5}{2}}} + \frac{\frac{12(a^2 + b^2 + c^2)}{(a^2 + b^2 + c^2)^{\frac{5}{2}}}}{\mathbf{p}} = 0.$$

A similar calculation may be performed for each of the other sets of twelve points until the entire sphere is covered. Thus the effective field due to the ions in the sphere vanishes:

$$E_{eff} = 0$$
.

Recalling the approximation made earlier, that the difference between  $\underline{\mathbf{E}}_{\text{eff}}$  and  $\underline{\mathbf{E}}$  is due only to the contributions of the matter contained within the sphere, one obtains

$$\underline{\mathbf{E}}\mathbf{eff}-\underline{\mathbf{E}}=\underline{\mathbf{0}}-(-\frac{4\pi}{3}\ \underline{\mathbf{P}})\ ,$$

or

$$\underline{\mathbf{E}}_{\mathrm{eff}} = \underline{\mathbf{E}} + \frac{4\pi}{3} \underline{\mathbf{P}}. \tag{1}$$

Let  $\underline{\mathbf{u}}_+$ ,  $+\mathbf{Z}\mathbf{e}$ ,  $\underline{\mathbf{e}}_+$ ,  $\underline{\mathbf{p}}_+$  be respectively the displacement, ionic charge, atomic polarizability, and effective dipole moment of the positive ions. Then

$$\underline{p}_{+} = \mathbf{Z}\underline{\mathbf{e}}\underline{\mathbf{u}}_{+} + \alpha_{+} \underline{\mathbf{E}}_{eff} . \tag{2}$$

Similarly, for the negative ions,

$$\underline{p} = - \underline{Z}\underline{e}\underline{u} + \underline{a} \underline{E}\underline{e}\underline{f}. \qquad (3)$$

If one lets  $V_0$  be the volume of a lattice cell, then the polarization P is

$$\underline{\mathbf{P}} = \frac{1}{V_0} \left[ \mathbf{Z} e(\underline{\mathbf{u}}_+ - \underline{\mathbf{u}}_-) + (\mathbf{a}_+ + \mathbf{a}_-) \underline{\mathbf{E}}_{eff} \right], \tag{4}$$

for there are two ions, one positive and one negative, per lattice cell. Eliminating  $\mathbf{E}_{\mathrm{eff}}$  by using (1), and introducing

$$\underline{\mathbf{w}} = \left(\frac{\mu}{V_0}\right)^{\frac{1}{2}} \left(\underline{\mathbf{u}}_+ - \underline{\mathbf{u}}_-\right), \tag{5}$$

where

$$\mu = \frac{M_+ M_-}{M_+ + M_-}$$

is the reduced mass of the positive and negative ions of molecular weight  $M_+$  and  $M_-$  respectively, gives

$$P = b_{21} w + b_{22} E$$
, (6)

where

$$b_{21} = \frac{\frac{Ze}{(\mu V_0)^{\frac{1}{2}}}}{1 - \frac{4\pi}{3}(\frac{a_+ + a_-}{V_0})}, \quad b_{22} = \frac{(\frac{a_+ + a_-}{V_0})}{1 - \frac{4\pi}{3}(\frac{a_+ + a_-}{V_0})}. \quad (7)$$

Equation (6) represents one of the lattice equations.

To derive the other lattice equation, one notes that when the positive and negative ions are relatively displaced, the overlap potential gives rise to a force on the ions which can be taken as directly proportional to the relative displacement  $\underline{\mathbf{u}}_+ - \underline{\mathbf{u}}_-$  between the ions for small displacements. Thus, the force on a positive ion can be written

$$- k (\underline{u}_{+} - \underline{u}_{-})$$

and the corresponding force on a negative ion,

$$k(\underline{u}_+ - \underline{u}_-)$$
,

where the coefficient k is a scalar as a result of the tetrahedral symmetry of the crystal lattice. Taking into account the forces exerted on the ions by  $\mathbf{E}_{\text{eff}}$ , as well, enables one to write the equations of motion for the positive and negative ions as

$$M_{+} \underline{\ddot{u}}_{+} = -k (\underline{u}_{+} - \underline{u}_{-}) + Ze \underline{E}_{eff}$$
,

$$M_{\ddot{u}} = k (u_{+} - u_{-}) - Ze E_{eff}$$
,

respectively. Upon solving these equations simultaneously, and using (1), (5), and (6), one obtains the remaining lattice equation (the equation of motion for the lattice)

$$\underline{\ddot{\mathbf{w}}} = \mathbf{b}_{11} \ \underline{\mathbf{w}} + \mathbf{b}_{12} \ \underline{\mathbf{E}}, \tag{8}$$

where

$$b_{11} = -\frac{k}{\mu} + \frac{\frac{4\pi}{3} \frac{(Ze)^2}{\mu V_0}}{1 - \frac{4\pi}{3} (\frac{\alpha_+ + \alpha_-}{V_0})}, \quad b_{12} = \frac{\frac{Ze}{(\mu V_0)^{\frac{1}{2}}}}{1 - \frac{4\pi}{3} (\frac{\alpha_+ + \alpha_-}{V_0})}. \quad (9)$$

#### B. Macroscopic Considerations

The optical lattice vibrations of long wavelengths (infrared) must satisfy the two lattice equations derived above:

$$\ddot{\mathbf{w}} = \mathbf{b_{11}} \ \mathbf{w} + \mathbf{b_{12}} \ \mathbf{E} \ , \tag{8a}$$

$$P = b_{21} w + b_{22} E$$
, (6a)

where  $b_{12} = b_{21}$ , as seen from equations (7) and (9). Substituting the

periodic solutions

$$\frac{\mathbf{E}(\mathbf{x}, \mathbf{y}, \mathbf{z}, t) = \mathbf{E}_0(\mathbf{x}, \mathbf{y}, \mathbf{z})}{\mathbf{w}(\mathbf{x}, \mathbf{y}, \mathbf{z}, t) = \mathbf{w}_0(\mathbf{x}, \mathbf{y}, \mathbf{z})}$$

$$\mathbf{P}(\mathbf{x}, \mathbf{y}, \mathbf{z}, t) = \mathbf{P}_0(\mathbf{x}, \mathbf{y}, \mathbf{z})$$

where  $\omega$  is the angular frequency, into the lattice equations (8a) and (6a), and then solving for P gives

$$\underline{\mathbf{P}} = \left[\mathbf{b}_{22} + \frac{\mathbf{b}_{12}\mathbf{b}_{21}}{-\mathbf{b}_{11} - \omega^2}\right] \underline{\mathbf{E}} . \tag{10}$$

Since the dielectric constant is defined through

$$\underline{\mathbf{D}} = \mathbf{E} + 4\pi \ \underline{\mathbf{P}} = \boldsymbol{\epsilon} \ \mathbf{E} \ , \tag{11}$$

where  $\underline{D}$  is the electric displacement, one can solve (11) for  $\underline{P}$  and compare it with (10), to obtain the following expression for the dielectric constant:

$$\epsilon = 1 + 4\pi b_{22} + \frac{4\pi b_{12} b_{21}}{-b_{11} - \omega^2}$$
 (12)

This dispersion formula may be written as

$$\epsilon = \epsilon_{\infty} + \frac{\epsilon_0 - \epsilon_{\infty}}{1 - \left(\frac{\omega}{\omega_0}\right)^2} , \qquad (13)$$

if one sets

$$b_{11} = -\omega_0^2, (14)$$

$$b_{12} = b_{21} = \left(\frac{\epsilon_0 - \epsilon_{\infty}}{4\pi}\right)^{\frac{1}{2}} \omega_0,$$
 (15)

$$b_{22} = \frac{\epsilon_{\infty} - 1}{4\pi} \quad , \tag{16}$$

where  $\omega_0$  is called the <u>angular infrared dispersion frequency</u>,  $\epsilon_0$  the static dielectric constant, and  $\epsilon_{\infty}$  the <u>high frequency dielectric constant</u>.

One can now relate the b-values given by the microscopic theory in equations (7) and (9) with those given by the macroscopic considerations in (12) to (16). Thus comparing the right hand side of (7) with (16) leads to

$$\frac{4\pi}{3} \left(a_{+} + a_{-}\right) = \left(\frac{\epsilon_{\infty} - 1}{\epsilon_{\infty} + 2}\right) \vee_{0} \tag{17}$$

when b22 is eliminated. Combining the left hand side of (7) with (15) gives

$$\frac{\left(\frac{Ze}{\mu}\right)^{2}}{\left[1-\frac{4\pi}{3}\left(\frac{\alpha++\alpha_{-}}{V_{0}}\right)\right]^{2}} = b_{12}^{2} = \omega_{0}^{2}\left(\frac{\epsilon_{0}-\epsilon_{\infty}}{4\pi}\right),$$

which enables one to write  $b_{11}$  given in equation (9) as

$$b_{11} = -\frac{k}{\mu} + \frac{4\pi}{3} \omega_0^2 \left( \frac{\epsilon_0 - \epsilon_{\infty}}{4\pi} \right) \left[ 1 - \frac{4\pi}{3} \left( \frac{\alpha_+ + \alpha_-}{V_0} \right) \right]. (18)$$

Eliminating the atomic polarizabilities by the use of (17), and noting that (14) allows one to set  $b_{11} = -\omega_0^2$ , one obtains

$$\omega_0 = \sqrt{\frac{k}{\mu} \left( \frac{\epsilon_{\infty} + 2}{\epsilon_0 + 2} \right)} . \tag{19}$$

Thus, the infrared dispersion frequency should vary as the inverse square root of the reduced mass.

If one now considers an isotope of the ionic crystal made up of ions of atomic weight M<sup>1</sup><sub>+</sub> and M<sup>1</sup><sub>-</sub>, equation (19) predicts that the dispersion frequency should shift inversely with the square root of the new reduced mass,

$$\mu' = \frac{M_{+}' M_{-}'}{M_{+}' + M_{-}'}$$

to a new value  $\omega_0$ . From the definition of  $\omega_0$  as  $\sqrt{-b_{11}}$  in equation (14), and the definition of  $b_{11}$  in equation (9), it is seen that  $\omega_0$  varies as  $\sqrt{1/\mu}$ ,

depending otherwise only on quantities (k, Z,  $V_0$ ,  $a_+$ ,  $a_-$ ) which vary at most only very slightly with isotopic mass. Thus, one may calculate the ratio of  $\omega_0$  to  $\omega_0$ , and obtain

$$\frac{\omega_0}{\omega_0!} = \sqrt{\frac{\mu!}{\mu}} \tag{20}$$

or

$$\frac{\lambda_0}{\lambda_0!} = \sqrt{\frac{\mu}{\mu!}}$$
 (21)

which says that the ratio of the respective infrared dispersion wavelengths of two isotopes is equivalent to the square root of the reduced masses. It is this prediction which will be of primary interest in this thesis.

#### THEORY OF THE EXPERIMENT<sup>3,6</sup>

The dispersion formula (13) derived in the previous section only gives qualitative agreement with experimental results in the neighborhood of the infrared dispersion (or absorption) frequency  $\omega_0$  (or wavelength  $\lambda_0$ ) for it predicts that  $\epsilon$  should proceed to  $+\infty$  when  $\omega_0$  is approached by the frequency from below and  $-\infty$  when approached from above. This result does not agree with the experimental result that  $\epsilon$  remains finite in this region. Hence, for the purpose of analyzing empirical data in the neighborhood of  $\omega_0$ , one is led to derive a dispersion formula which takes account of the energy dissipation in the crystal in an ad hoc way. A simple damping term can be introduced into the lattice equation of motion

$$\ddot{\mathbf{w}} = \mathbf{b_{11}} \ \mathbf{w} + \mathbf{b_{12}} \ \mathbf{E} \tag{8a}$$

to obtain an equation of motion with damping:

$$\underline{\ddot{\mathbf{w}}} = \mathbf{b}_{11} \ \underline{\mathbf{w}} - \gamma \ \underline{\dot{\mathbf{w}}} \ + \mathbf{b}_{12} \ \underline{\mathbf{E}}, \tag{22}$$

where  $\gamma$  is a positive constant with the dimension of frequency. The additional term represents a force proportional to the velocity  $\dot{\underline{w}}$  and always opposed to the direction of the motion. Substituting the complex periodic solutions of the type used before, namely,

$$\frac{\mathbf{w} = \mathbf{w}_0}{\mathbf{E} = \mathbf{E}_0}$$
 \rightarrow e^{-i\omega t}

into (8a) and (22), one obtains respectively

$$-\omega^2 \underline{w} = b_{11} \underline{w} + b_{12} \underline{E},$$
 (23)

$$-\omega^2 = (b_{11} + i\omega\gamma) + b_{12} = .$$
 (24)

Comparing these equations, one sees that the addition of the damping term is equivalent to the replacement of  $b_{11}$  by  $b_{11} + i\omega\gamma$ . Thus the dispersion formula obtained in the previous section (see equations (12) and (13)) becomes

$$\epsilon = 1 + 4\pi \cdot b_{22} + \frac{4\pi b_{12}b_{21}}{-b_{11} - i\omega\gamma - \omega^{2}}$$

$$= \epsilon_{\infty} + \frac{\epsilon_{0} - \epsilon_{\infty}}{1 - (\frac{\omega}{\omega_{0}})^{2} - i(\frac{\omega}{\omega_{0}})(\frac{\gamma}{\omega_{0}})}$$
(25)

To make use of the dispersion formula (25) in this thesis, the transmission coefficient (or transmittance) must first be derived. Consider the reflection and transmission of plane waves of frequency  $\omega$  by a plane film of thickness d at normal incidence. If x is the direction of incidence with the origin taken at the incident side of the film,  $\overline{n}$  the complex index of refraction, and c the velocity of light in a vacuum, then the electric field can be written as

$$(A e^{i\omega x/c} + B e^{-i\omega x/c}) e^{-i\omega t}$$

on the incident side of the film,

$$(C e^{i\omega nx/c} + D e^{-i\omega nx/c}) e^{-i\omega t}$$

within the film, and

$$E e^{i\omega(\frac{x}{c}-t)}$$

on the far side. In the above expressions A, B,..., E are the complex amplitudes of the field components. The corresponding expressions for the magnetic field are:

(A 
$$e^{i\omega x/c}$$
 - B  $e^{-i\omega x/c}$ )  $e^{-i\omega t}$ ,  
 $\overline{n}$  (C  $e^{i\omega \overline{n}x/c}$  - D  $e^{-i\omega \overline{n}x/c}$ )  $e^{-i\omega t}$ ,  
E  $e^{i\omega(\frac{x}{c}-t)}$ .

Imposing the requirement that the electric and magnetic fields be continuous across the film boundaries gives four linear homogeneous equations in the coefficients A, B, ..., E:

A + B - C - D = 0,  
A - B - 
$$\overline{n}$$
 C +  $\overline{n}$  D = 0,  

$$e^{i\omega\overline{n}d/c} \cdot C + e^{-i\omega\overline{n}d/c} \cdot D - e^{i\omega d/c} \cdot E = 0,$$

$$\overline{n} e^{i\omega\overline{n}d/c} \cdot C + \overline{n} e^{-i\omega\overline{n}d/c} \cdot D - e^{i\omega d/c} \cdot E = 0.$$

These equations may be solved immediately for the ratio E/A:

$$\frac{E}{A} = \frac{4 \, \overline{n} \, e^{-i\omega d/c}}{(1 + \overline{n})^2 \, e^{-i\omega n d/c} - (1 - \overline{n})^2 \, e^{i\omega n d/c}} . \tag{26}$$

For very thin films such that  $\omega d/c << 1$  (for the films used in this work, this ratio turns out to be about  $10^{-2}$ ), the exponentials in (26) can be expanded to find

$$\frac{E}{A} = \frac{1}{(1 + i\omega d/2c)(1 - \overline{n}^2)}$$
, (27)

where terms of higher order than  $\omega d/c$  have been dropped. Since the radiation intensity is proportional to the square of the absolute value of the electric (or magnetic) field, and the transmittance T is defined as the intensity ratio of the emerging to the incident radiation, one obtains

<sup>\*</sup>Several algebraic errors occur in the treatment of reference (3). The result of equation (28) is, however, obtained correctly.

$$T = \left| \frac{E}{A} \right|^2 = \frac{1}{1 + i\omega d/2c (\overline{n}^{*2} - \overline{n}^2)}$$
, (28)

where again terms of higher order than  $\omega d/c$  have been dropped. Minimum transmittance occurs when the denominator in (28) is maximum, i.e. at that frequency for which

$$i\omega(\overline{n}^{*2} - \overline{n}^2) = i\omega(\epsilon^* - \epsilon)$$
 (29)

is a maximum. Substituting the expression for  $\epsilon$  from (25) gives

$$i\omega(\epsilon^* - \epsilon) = 2\gamma \left(\frac{\epsilon_0 - \epsilon_{\infty}}{\omega_0^2}\right) \frac{\omega^2}{(\omega_0^2 - \omega^2)^2 + \gamma^2 \omega^2}.$$
 (30)

From the condition that at the maximum

$$\frac{\mathrm{d}}{\mathrm{d}\omega} \left[ \mathrm{i}\omega \left( \epsilon^* - \epsilon \right) \right] = 2 \gamma \left( \frac{\epsilon_0 - \epsilon_\infty}{\omega_0^2} \right) \frac{2\omega \left( \omega_0^2 + \omega^2 \right) \left( \omega_0^2 - \omega^2 \right)}{\left[ \left( \omega_0^2 - \omega^2 \right)^2 + \gamma^2 \omega^2 \right]^2} = 0,$$

one sees that expression (29) has a maximum at the frequency  $\omega = \omega_0$ . Hence, for sufficiently thin films, the transmittance T has a minimum which occurs at the infrared dispersion frequency  $\omega_0$ .

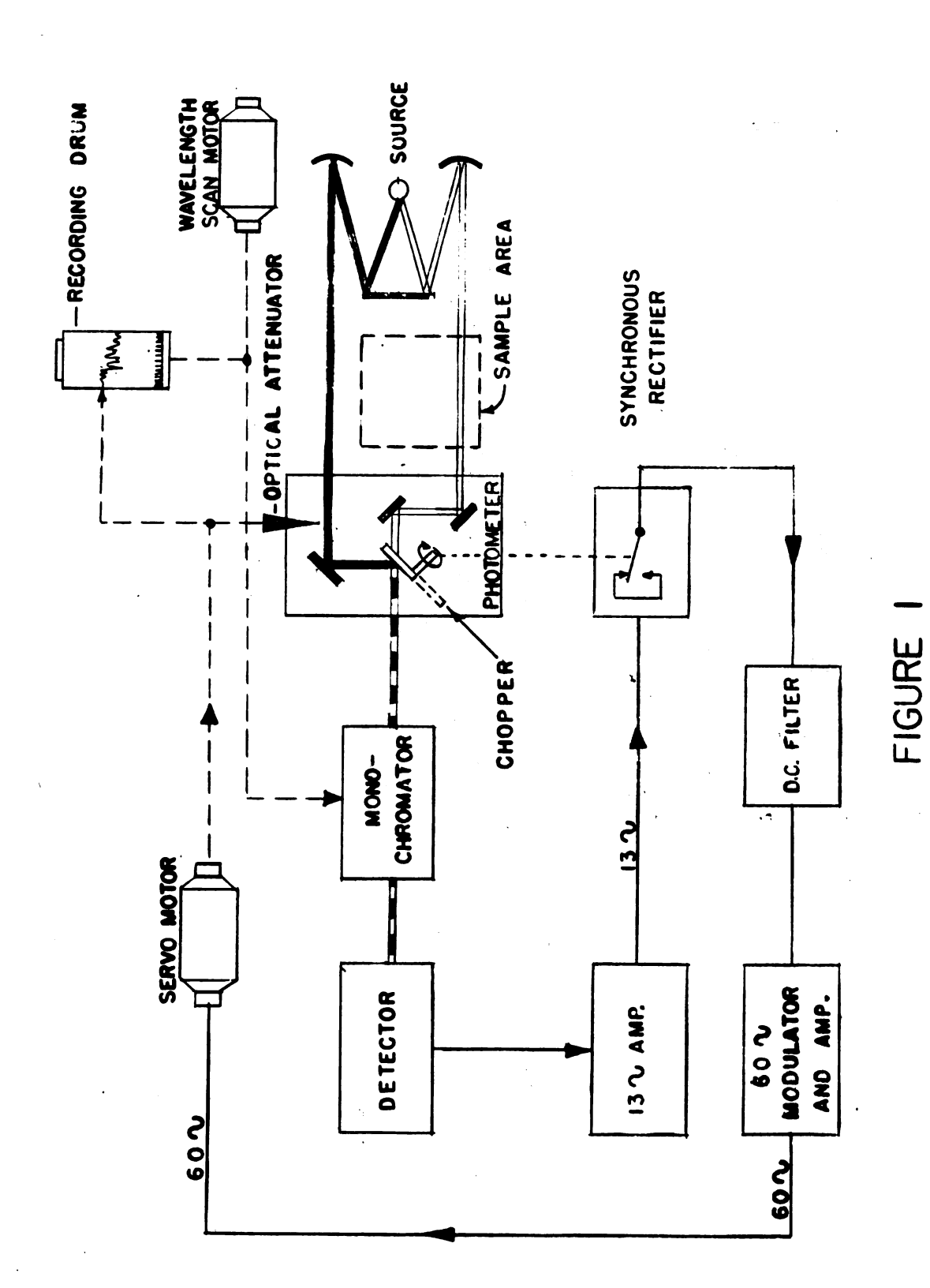
#### APPARATUS AND METHOD

#### A. Infrared Spectrophotometer

The transmission spectra were obtained by using a Perkin-Elmer model 137 recording spectrophotometer ("Infracord") which operated on the double-beam optical-null principle. The optics (potassium bromide) used in this instrument permitted the scanning of the infrared spectrum in the region from 12.5 $\mu$  to 25 $\mu$ , and provided a continuous record of the infrared transmittance of a sample as a function of the wavelength of the incident radiation. The specifications of the instrument, as supplied by the manufacturer, included a wavelength accuracy of  $\pm$  0.03 $\mu$ , a wavelength reproducibility of  $\pm$  0.02 $\mu$ , and a transmission reading accuracy and reproducibility of  $\pm$  1%.

A block diagram of the instrument is shown in Figure 1. The radiation produced by the source is divided into two beams. One beam passes through the sample which absorbs certain characteristic wavelengths; the other serves as a reference. The two beams are recombined by a rotating semicircular sector mirror or chopper into a single beam consisting of alternate pulses of sample and reference radiation. The monochromator disperses the combined radiation into its constituent wavelengths and successively transmits small wavelength intervals to the detector (an evacuated thermocouple). If the energy in both beams is equal, the pulses from the two beams are equal in intensity. The result is that the thermocouple produces a direct voltage which is not amplified by the a-c amplifier of the instrument.

When, at the characteristic wavelengths of the sample, the intensity of the sample beam is reduced by absorption, the two signals are unequal and the combined beam flickers at 13 cps, the rotational frequency of the chopper. The amplitude of the variation is proportional to the difference



INFRACORD BLOCK DIAGRAM

in intensity of the two beams, and the phase depends on which of the two beams has the higher energy.

The pulsating portion of the light beam is converted by the detector to an alternating voltage and amplified by the 13-cps amplifier. This alternating signal is called the error signal and is proportional to the difference between the sample-beam intensity and the reference-beam intensity. It is then converted to a 60-cps alternating voltage operating the servo motor which moves the marking pen and an optical attenuator placed in the reference beam until the two beam intensities are equalized.

#### B. Analysis of the Lithium Hydride Samples

The lithium hydride and lithium deuteride samples were obtained in powdered form with the help of Mr. J. B. Milgram of the Foote Mineral Company and Mr. R. E. Miner of Metal Hydrides Incorporated, respectively. In both cases, the samples were made from natural lithium depleted in lithium-6. Their approximate analysis by weight, as supplied by the manufacturers, is tabulated below:

Sample	<u>Li</u> 6	Li <sup>7</sup>	$\overline{\mathbf{H_I}}$	H²
LiH <sup>1</sup>	3%	97%	100%	-
LiH <sup>2</sup>	3%	97%	2%	98%

The samples of lithium-6 hydride and lithium-6 deuteride were obtained in lump form through the aid of Dr. P. S. Baker of the Stable Isotopes Research and Production Division of Oak Ridge National Laboratory. From the data furnished by the supplier, the following analyses can be given with these clarifications:

- 1. The spectrographic results reported are semiquantitative estimates and should not be interpreted or construed to be precise quantitative determinations;
- 2. < -No spectrum line visible. Probably absent, definitely less than value given.

Lithium-6 Hydride (Li<sup>6</sup>H<sup>1</sup>)
Lot No. SS 5(e)

Grams li gram ma	thium per terial	Isotope	Atomic Percent
Exp.	Calc.	Li <sup>6</sup>	95.64
0.8470	0.8574	Li <sup>7</sup>	4.36
		$H^1$	100.0000
		H <sup>2</sup>	0.0000

## Spectrographic Analysis

Weight Percent
. 028
< .004
< .004
.0004
.003
< .002
.004
< .0002
< .0006
< .002
< .0001
.001
.002
.0004
< .0004
. 006
.001

Si	.004
Sn	< .002
Sr	< .001
V	< .001
<b>Z</b> n	< .1
Nb	< .01

## Lithium-6 Deuteride (Li<sup>6</sup>H<sup>2</sup>)

Lot No. SS 5(f)

Grams lithium per gram material		Isotope	Atomic Percent
Exp.	Calc.	Li <sup>6</sup>	95.62
0.7473	0.7527	Li <sup>7</sup>	4.38
		$H^1$	2.321
		H <sup>2</sup>	97.6786

## Spectrographic Analysis

Element	Weight Percent
Na	< .004
Ca	< .004
K	.004
Ag	.001
Al	.002
В	< .002
Ba	.002
Be	< .0002
Cd	< .0006
Co	< .002
Cr	.0001
Cu	.0015
Mg	.002
Mn	. 0002
Mo	< .0004
Ni	. 006
${f P}{f b}$	.0008
Si	.002
Sn	< .002

Sr	<.001
V	<.001
<b>Z</b> n	<.1
Nb	< .01

The difference between the experimental and calculated values for grams lithium per gram material indicates that the material contained some impurities, most probably, in the form of lithium oxide, hydroxide, or carbonate.

#### C. Film Preparation

As has been previously mentioned, an evaporation technique was chosen to prepare the thin films (thickness less than lµ) of lithium hydride. Preparing thin films always poses difficulties; in the present case, the problem was greatly magnified by the rapidity with which lithium hydride reacts with air of even low humidity to form lithium oxide (Li<sub>2</sub>O), lithium hydroxide (LiOH or LiOH·H<sub>2</sub>O), and lithium carbonate (Li<sub>2</sub>CO<sub>3</sub>). Moreover, lithium hydride powder reacts explosively with water, and there is a tendency for lithium hydride dust to explode in humid air, or even in dry air, upon ignition by static electricity. The dust is also extremely irritating to the mucous membranes and skin, causing a severe skin reaction in some individuals. Fortunately, handling in a dry box eliminates most of these hazards.

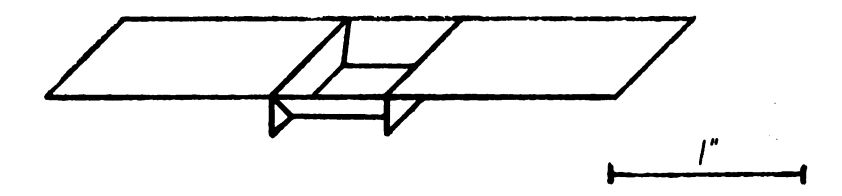
### 1. Preparation of the Composite Samples

Because the composition of only the Li<sup>6</sup>H<sup>1</sup> and Li<sup>6</sup>H<sup>2</sup> samples was accurately known, composite samples were made up only from these samples. In an argon dry box, a suitable amount (about 100 mg) of one of the compounds was placed in a weighing bottle, and weighed to the nearest 0.1 mg; then an estimated amount of the other compound

was added to give approximately the desired composition, and accurate weighing was again carried out. By this means, values accurate to at least 3 significant figures could be obtained of the composition of the sample by weight. The composite sample was then ground to a powder in an agate mortar.

#### 2. Evaporation of the Sample

The boats used for melting and evaporating the lithium hydride samples were made out of molybdenum sheet stock into the form illustrated in Figure 2. The evaporating boats were loaded with the



Molybdenum Evaporating Boat

#### FIGURE 2

sample (about 1 mg) in an argon dry box, and then transferred to the vacuum chamber under the rays of an infrared heat lamp. Although the sample was exposed to the atmosphere for a minute or two in the latter step, it was found that the warming action of the heat lamp gave sufficient protection against moisture to the sample. When a pressure of about 10<sup>-4</sup> mm Hg had been attained in the vacuum chamber, the boat was heated by sending a current through it. The heating was carried out gradually by increasing the current at a rate of about 2 amp/min. This was necessary because of the outgassing of the molybdenum and liberation of some hydrogen from the sample which, if too rapid, would throw the sample from the boat. When the boat

began to glow a dull red, the sample melted and evaporated immediately.

#### 3. Film Protection

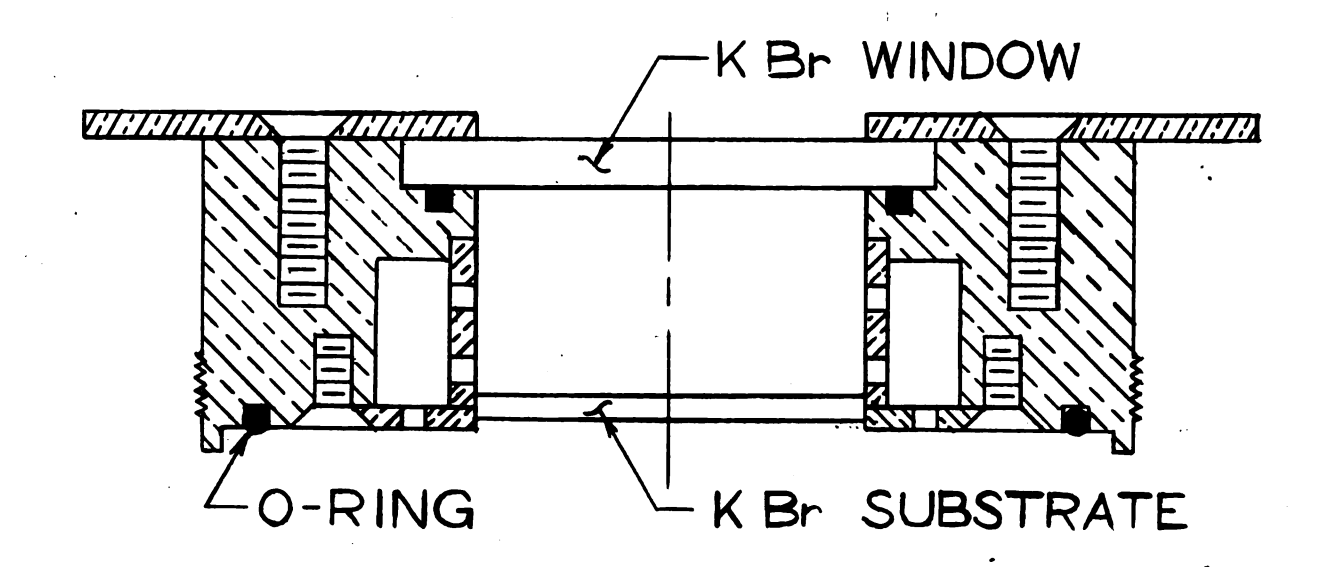
The lithium hydride sample was evaporated onto a blank of potassium bromide (KBr) 2 mm thick and 1 inch in diameter. At first, an attempt was made to protect the film by evaporating a layer of carbon over the film; however, it was found that moisture would quickly seep in at the edges and ruin the film, probably changing it to lithium hydroxide. A typical absorption spectrum of such a film is shown in Figure 8.

Consequently, a special vacuum-tight cell of two parts, illustrated in Figure 3, was designed and constructed. The cell body was constructed out of brass. KBr windows were used to allow the passage of the infrared radiation with a KBr blank (2 mm thick by 1 inch diameter) positioned to act as the substrate at the bottom of the upper part of the cell by two expansible rings. Silicone rubber 0-rings were used as the static seals. A circular chamber was made in the wall of the upper part to hold a dessicant to provide added protection against moisture.

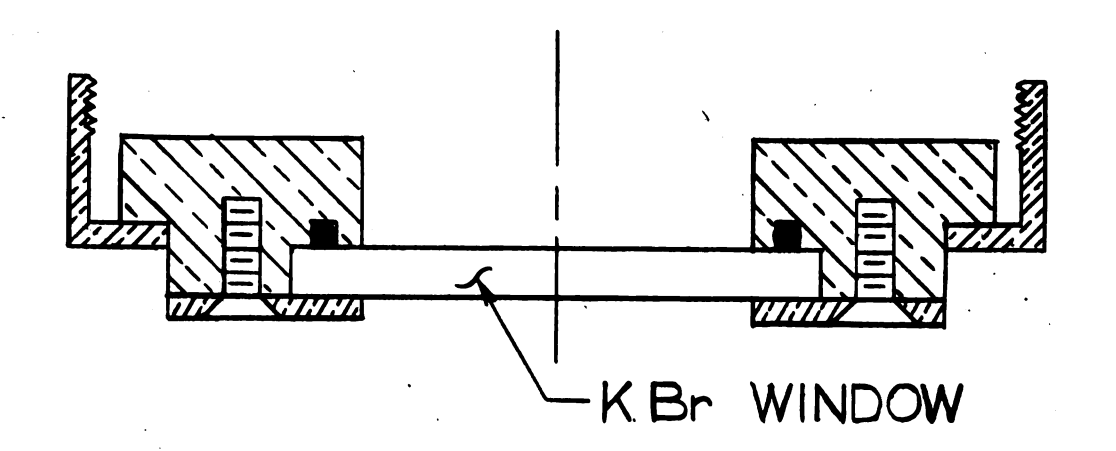
To take advantage of the double-beam optical-null principle of the "Infracord," a similar cell was constructed to be used in the reference beam. This reference cell is shown in Figure 4.

#### 4. Vacuum-Chamber Procedure

The arrangement of the components before an evaporation is shown in the foreground of the photograph of Figure 5. The upper part of the sample cell is placed about 5 inches above the molybdenum boat, and the lower part is put on a holder to one side. To provide a means of measuring the film thickness, a circular glass plate (6 mm by 57.5 mm)



# UPPER PART



LOWER PART

FIGURE 3
SAMPLE CELL

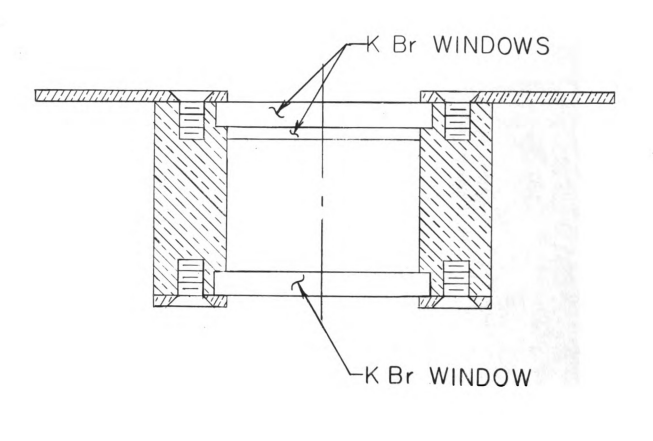


FIGURE 4
REFERENCE CELL

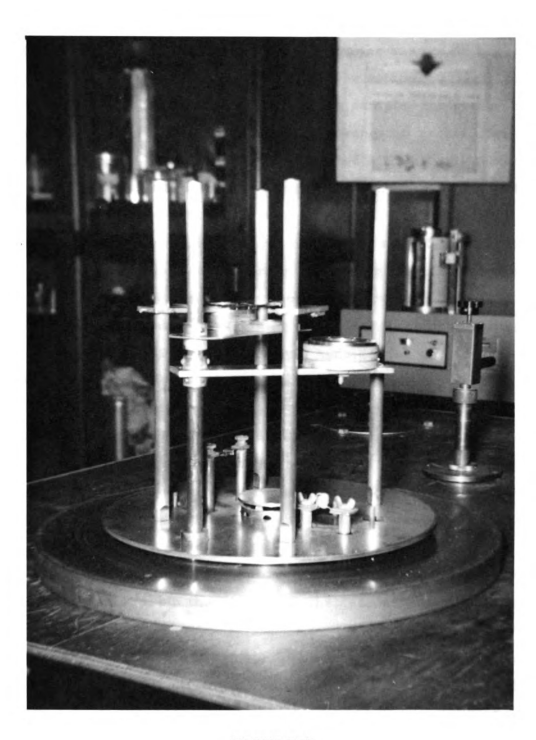


FIGURE 5
VIEW OF EXPERIMENTAL SETUP

is set next to the cell. Both the lower part and the glass plate rest on supports fastened to a rod inserted through the base plate of the vacuum chamber in such fashion that it may be rotated, raised, or lowered externally. After evaporation of the sample, the glass plate is rotated to one side and positioned above a tungsten basket coated with heat conducting alundum cement and filled with silver (or alum-The lower cell part is rotated beneath the upper part and raised to make contact with the 0-ring. The entire cell assembly is then raised and the 0-ring is compressed so that a tight seal results. Silver (or aluminum) is now evaporated onto the glass plate so that its entire surface is covered by a layer several microns thick. This layer not only provides a means of obtaining excellent interference fringes but at the same time protects the lithium hydride film for several hours. Air can now be passed into the chamber without damaging the film, since the cell is held tightly closed by atmospheric pressure. As an additional precaution against leaking at the seal between the cell parts, a circular band can be screwed tight (see Figure 3).

A variation of the above procedure is to allow helium or nitrogen to enter the chamber with the cell open instead of passing air into the vacuum chamber and keeping the cell interior in a vacuum. This alternative procedure should minimize leaks into the cell and provide better heat transfer from the film; nevertheless, no difference was noticed in the spectra.

The above technique for protecting a hygroscopic film is admittedly complicated and time-consuming. More efficient means can, no doubt, be found, but the procedure described seemed to be the quickest and best way to obtain good results with the equipment and facilities available.

# D. Measurement of Film Thickness<sup>8,9</sup>

A multiple-beam interference technique was used to measure the thickness of the evaporated films. In the method used, a film AB (see Figure 6) was deposited on part of a flat glass surface ABC. The entire flat was then covered with an opaque coating of silver (or aluminum) DEFG which was evaporated from a tungsten wire basket coated with alundum cement. The step EF equaled the thickness d of the film. A lightly silvered (or aluminized) flat HI was then brought close to the combination on AC to produce a wedge-shaped film of air between the metallized surfaces. When the assembly was illuminated from above with sodium light, back-reflected Fizeau fringes or fringes of constant thickness were formed. The coating of the film and the remainder of the flat AC with the opaque film DEFG automatically eliminated phase-change effects which would give faulty results if transmission fringes were used.

For normal observation with sodium light of wavelength  $\lambda$ , the condition for bright fringes is

$$2 \text{ n d'} = (m + 1/2) \lambda$$

or, since the index of refraction n is essentially unity for air,

$$2 d' = (m + 1/2) \lambda$$

where m is an integer, and d' is the thickness of the air film. This equation requires that d' should change by  $\lambda/2$  in going from one fringe to the next. Measuring the shift  $\Delta x$  of the fringes crossing the step EF and the distance x between fringes, then allows one to write

$$d = EF = \Delta d' = (\lambda/2) (\Delta x/x)$$
.

where  $\Delta d^{i}$  is the change in thickness of the air film at the step EF.

As seen in the photograph of Figure 7, the dark fringes are better used in the measurements because of their narrowness. It was found that some measurements of the thickness d could be made with an accuracy of ± 20 angstroms with a traveling microscope by first photographing the fringes with Kodak hi-contrast copy (Microfile) in order that the dark fringes would be changed to light ones, and at the same time have their contrast improved. Most of the measurements, however, were accurate to only about ± 50 angstroms.

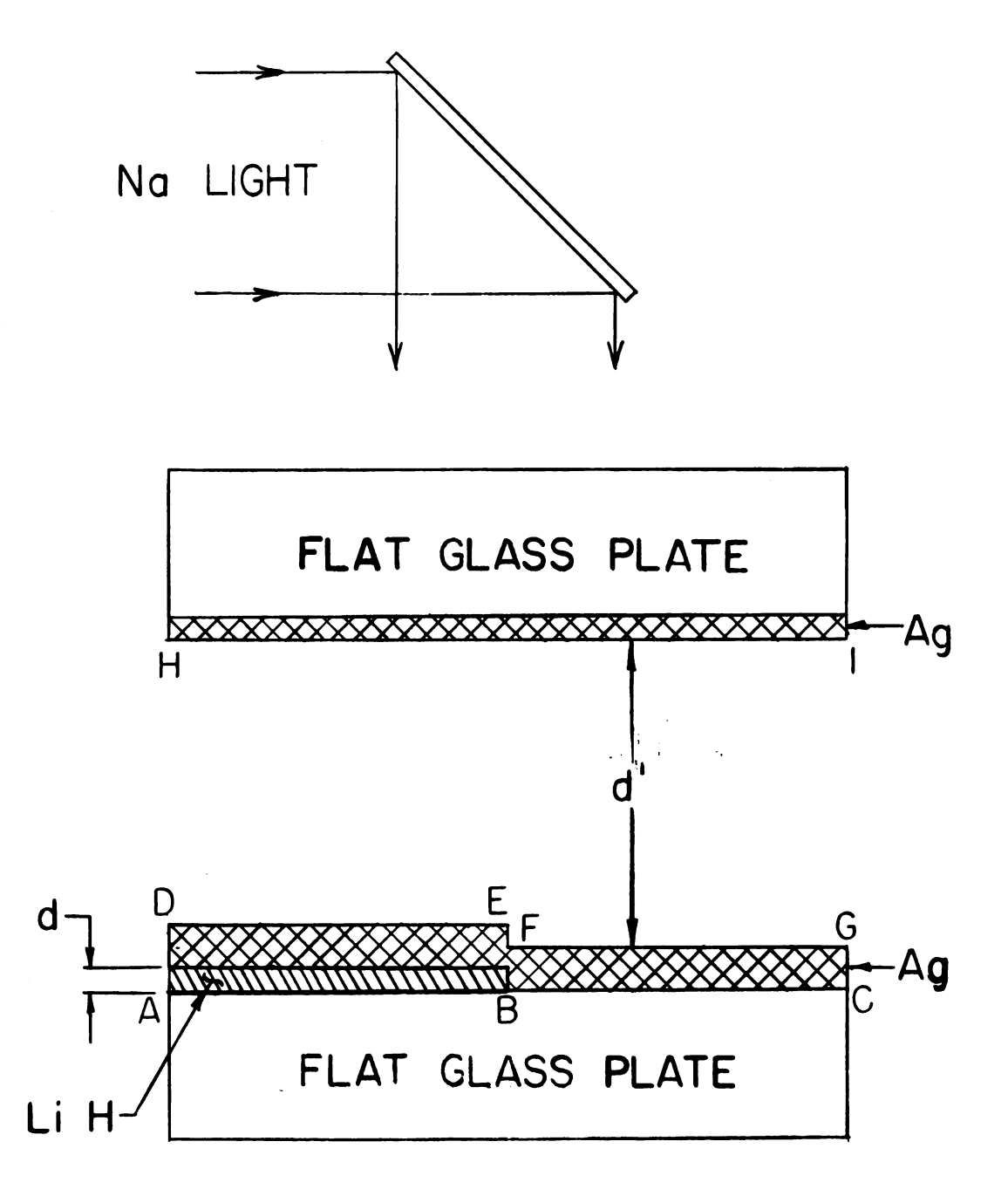


FIGURE 6
METHOD FOR OBTAINING FIZEAU FRINGES

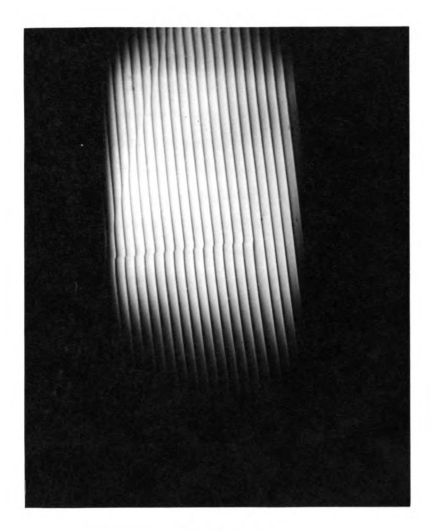


FIGURE 7  $\label{eq:figure 7}$  FIZEAU FRINGES FROM A STEP 0.0691  $\mu$  THICK

#### EXPERIMENTAL RESULTS

As mentioned before, the samples of lithium hydride had to be kept in a vacuum-tight cell to protect them from atmospheric moisture. If the sample cell containing an evaporated film of lithium hydride were placed in the sample beam of the "Infracord" at the same time that the reference beam was unobstructed, then the resulting spectrum would not only be that of the desired lithium hydride, but also of the KBr crystals used in the cell as windows and substrate. Although KBr is fairly transparent at lower wavelengths, its absorption of infrared radiation in the region beyond 20µ becomes large. This increase was especially noticeable in the present case because of the thick KBr windows that had to be used in the sample cell. Fortunately, the double-beam optical-null principle of the "Infracord" made it possible to cancel, in effect, the KBr absorption of the sample cell by inserting into the reference beam a unit (called the reference cell) with KBr windows whose total thickness approximated closely that of the sample cell. That this compensation was indeed possible is shown by the spectrum of Figure 9 when the cells were in their respective beams, as compared with an Io spectrum (nothing in either sample or reference beams) in Figure 10. The similar nature of the two curves, both in flatness and transmittance, shows that the undesirable KBr absorption was eliminated.

Energy pickup of scattered light by the detector, according to performance data supplied with the instrument, was less than 1% transmittance below 22μ and no more than 5% at a wavelength of 24.5μ.

Consequently energy pickup of this nature was neglected, since the spectrum of interest lay in the range from about 17 to 23μ.

Any sharp rises or falls in the spectra of Figures 8 to 12 should be regarded as caused by noise inherent in the "Infracord." Most of the

noise appeared to be due to the thermocouple used as the detector in the "Infracord."

### A. Effect of Isotopic Mass: Li<sup>6</sup>H<sup>1</sup>, Li<sup>6</sup>H<sup>2</sup>, Li<sup>7</sup>H<sup>1</sup>, Li<sup>7</sup>H<sup>2</sup>.

The spectra of these four compounds in the region from 12.5 to 25 $\mu$  are shown in Figure 11. In these curves, the infrared dispersion wavelength  $\lambda_0$  could be read to within 0.1 $\mu$ , and is probably accurate to  $\pm$  0.2 $\mu$ . These wavelengths are listed in Table I.

TABLE I
DISPERSION WAVELENGTHS AND REDUCED MASSES

Material	Dispersion Wavelength $\lambda_0$	Reduced Mass µ
Li <sup>6</sup> H <sup>1</sup>	$16.9 \pm 0.2 \mu$	0.864 amu
Li <sup>6</sup> H <sup>2</sup>	22.2	1.51
Li <sup>7</sup> H <sup>1</sup>	17.0	0.882
Li <sup>7</sup> H <sup>2</sup>	22.4	1.55

In Table II are listed the ratios of the dispersion wavelengths for various sample pairs as calculated from the observed values listed in Table I, or by using equation (21) in conjunction with the values for the reduced mass  $\mu$ , as listed in Table I, of the molecules composing the respective samples adjusted for isotopic impurity.

TABLE II

DISPERSION WAVELENGTH RATIOS

Sample Pair	Observed Ratio of Wavelengths	Square Root of Ratio of Reduced Masses
Li <sup>6</sup> H <sup>1</sup> -Li <sup>6</sup> H <sup>2</sup>	1.31 ± 0.02	1.32
$Li^7H^1-Li^7H^2$	1.32	1.33
$\mathrm{Li}^6\mathrm{H}^1$ - $\mathrm{Li}^7\mathrm{H}^1$	1.01	1.01
Li <sup>6</sup> H <sup>2</sup> -Li <sup>7</sup> H <sup>2</sup>	1.01	1.01

# B. Effect of Isotopic Composition: Li<sup>6</sup>[xH<sup>1</sup>, (1-x)H<sup>2</sup>]

The spectra of three mixtures composed of various amounts of  ${\rm Li}^6 {\rm H}^1$  and  ${\rm Li}^6 {\rm H}^2$  are shown in Figure 12. The infrared dispersion wavelengths  $\lambda_0$  for these composite films are listed in Table III, along with their average reduced masses.

TABLE III

DISPERSION WAVELENGTHS AND REDUCED MASSES

Compositio Li <sup>6</sup> H <sup>1</sup>	n by Weight Li <sup>5</sup> H <sup>2</sup>	Dispersion Wavelength $\lambda_0$	Average Reduced mass μ
100.0%	0.0%	$16.9 \pm 0.2 \mu$	0.864 amu
72.1	27.9	21.2	1.04
57.0	43.0	21.4	1,14
19.9	80.1	21.8	1.38
0.0	100.0	22.2	1.55
	100.0% 72.1 57.0 19.9	100.0% 0.0% 72.1 27.9 57.0 43.0 19.9 80.1	Li <sup>5</sup> H <sup>1</sup> Li <sup>5</sup> H <sup>2</sup> Wavelength $\lambda_0$ 100.0%     0.0%     16.9 ± 0.2 $\mu$ 72.1     27.9     21.2       57.0     43.0     21.4       19.9     80.1     21.8

The ratios of the dispersion wavelengths for some sample pairs are calculated and listed in Table IV by using the observed values in Table III or by using equation (21).

TABLE IV
DISPERSION WAVELENGTH RATIOS

Sample Pair	Observed Ratio of Wavelengths	Square Root of Ratio of Reduced Masses
1-2	$1.25 \pm 0.02$	1.09
2-3	1.01	1.05
3-4	1.02	1.10
4-5	1.02	1.04

### C. Measurement of Film Thickness

Film thicknesses, as measured by the multiple-beam interference method described in Section D of the chapter on Apparatus and Method, are listed on the graphs in Figures 11 and 12.

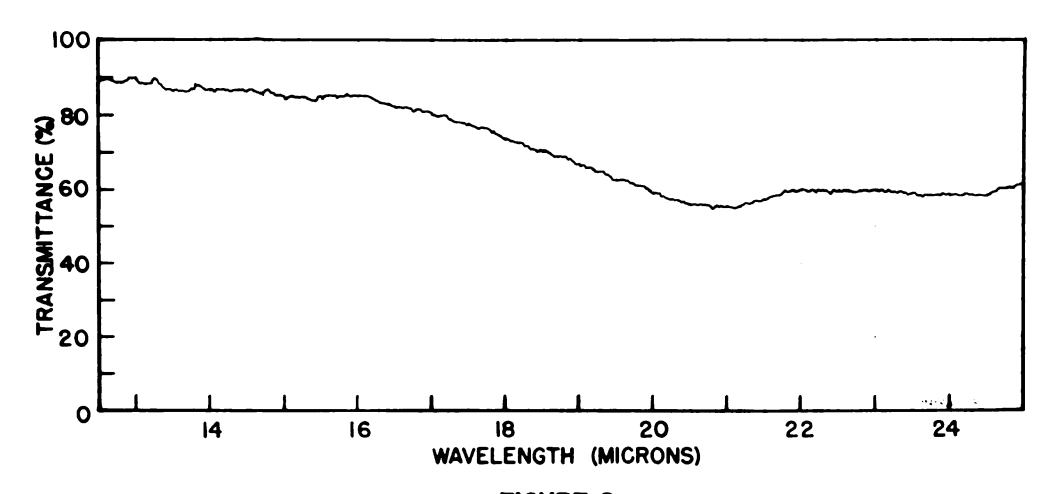
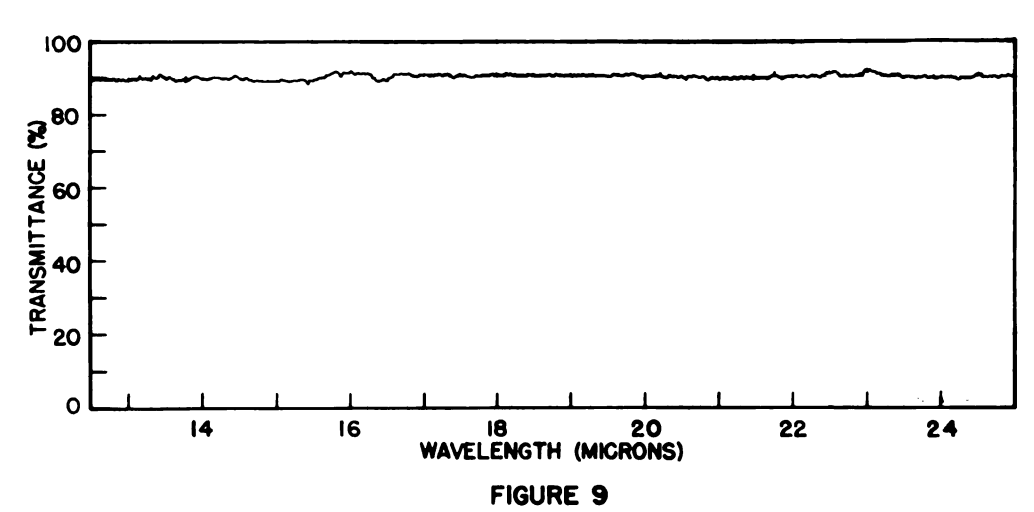


FIGURE 8
SPECTRUM OF LITHIUM HYDROXIDE FILM



IO SPECTRUM WITH CELLS IN RESPECTIVE BEAMS

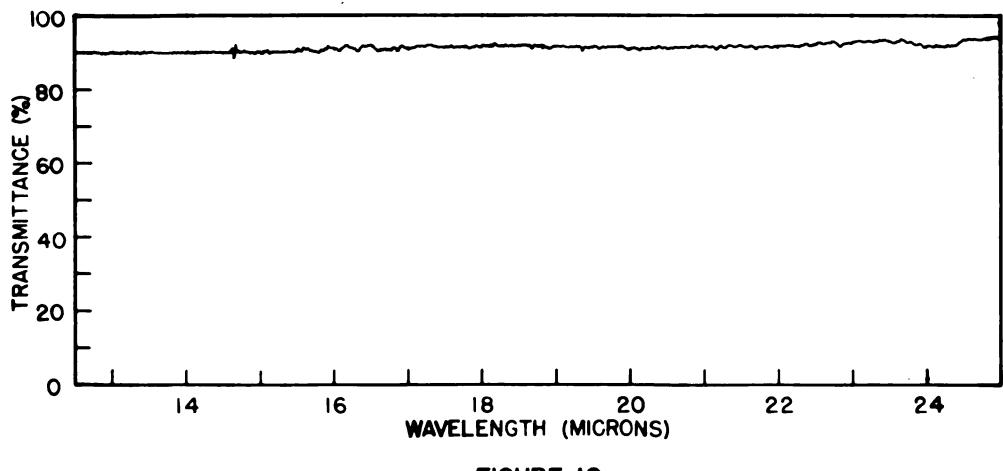
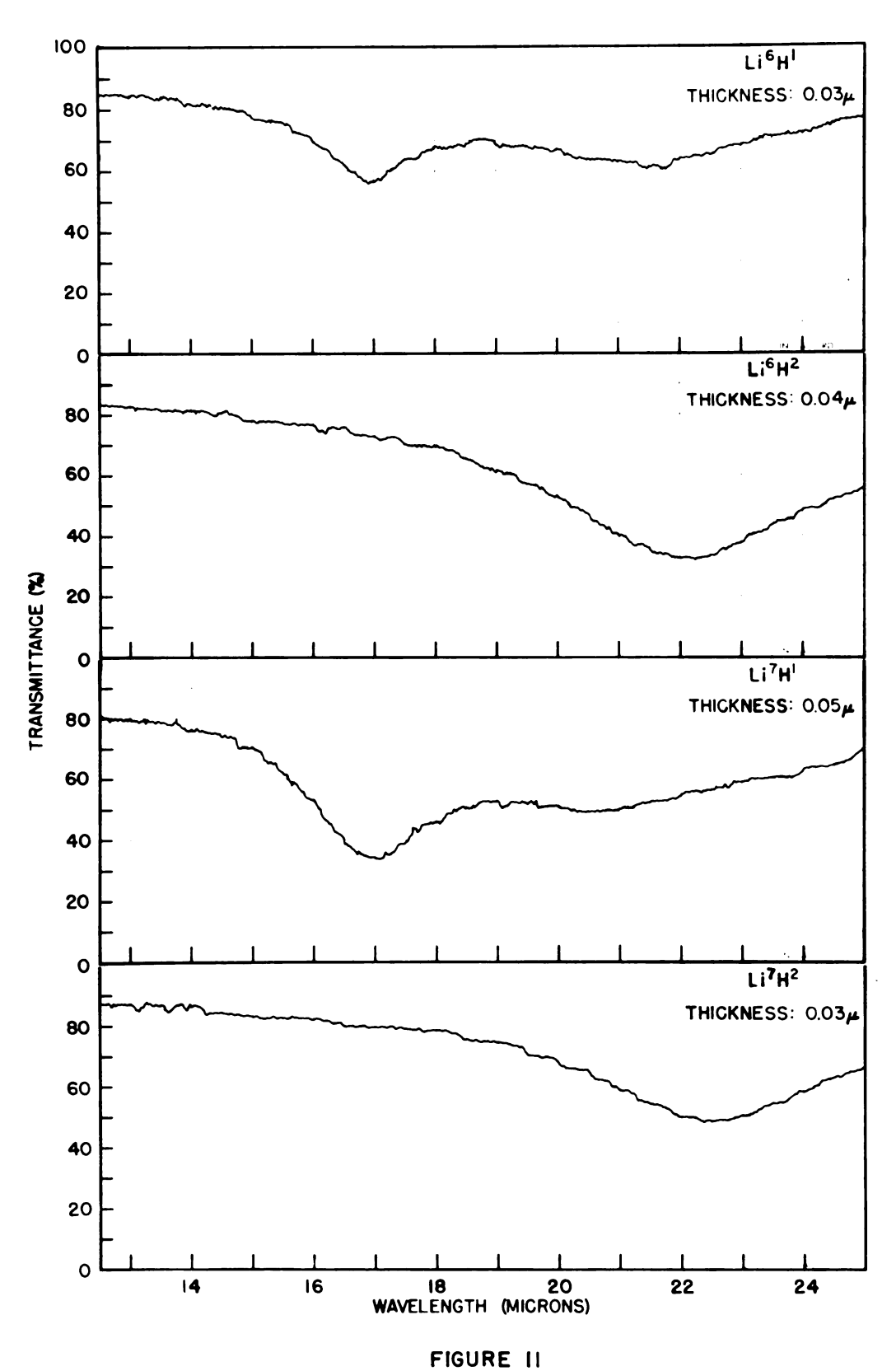


FIGURE 10
DOUBLE BEAM Io



SPECTRA OF LITHIUM-6 OR 7 IN COMBINATION WITH HYDROGEN-1 OR 2

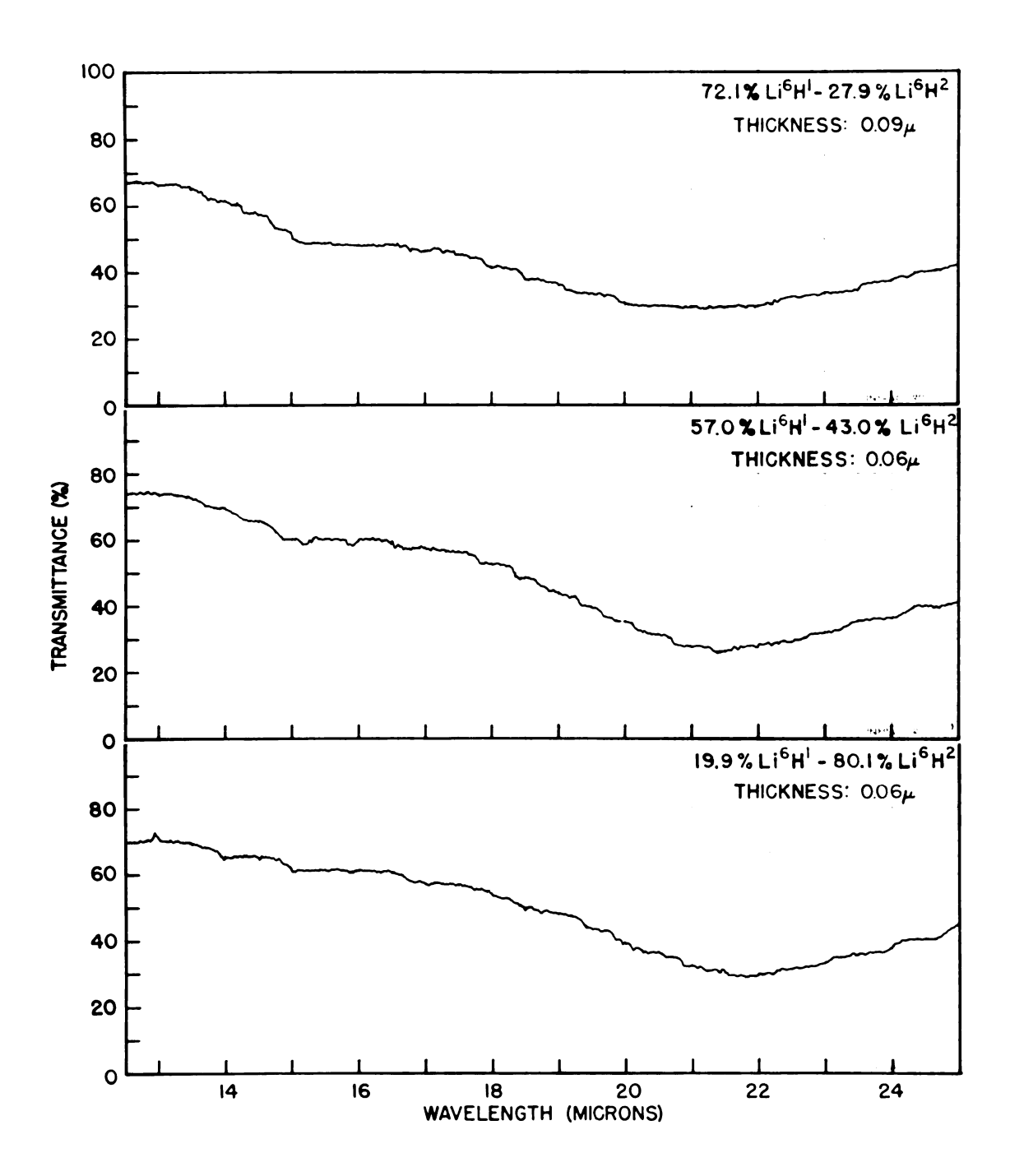


FIGURE 12
SPECTRA OF COMPOSITE FILMS

#### DISCUSSION OF RESULTS

The considerations of the previous section showed that by use of an appropriate reference cell the transmittance of only the lithium hydride film could be obtained as a function of wavelength. Thus, the dispersion wavelength of lithium hydride could be obtained. Although the absorption peaks were relatively broad, the position of the minimum transmittance could usually be determined to 0.  $l\mu$  for a particular film. But, as one would expect from the discussion in the Theory of the Experiment, the absorption peaks shift slightly as the thickness of the film is increased. Therefore, it is best that the film be quite thin (between 0.02 and 0.  $l\mu$ ) to get accurate results. Within this range of thickness the position of the absorption peak remained quite steady to within  $\pm$  0.  $2\mu$  or less. For thicknesses less than about 0.02 $\mu$ , it was found that the lithium hydride spectrum would become flat, indicating perhaps that the film was too thin to act as a real crystal lattice.

Some observations can immediately be made by comparing the spectrum of lithium hydride in the neighborhood of its dispersion wavelength with that of sodium chloride. Barnes and Czerny<sup>10</sup> found that for sodium chloride the absorption peak remained fixed at 61. lµ for films with a thickness of the order 0.1 to 1.0µ, whereas in the present work the peak remained fixed for thicknesses of the order 0.02 to 0.1µ. One interpretation of this observation is that the absorption coefficient of lithium hydride is about an order of magnitude greater than that of sodium chloride at the dispersion wavelength. Barnes and Czerny also found that the sodium chloride absorption peak shifted toward lower wavelengths with increase of thickness, where just the opposite appeared to occur in this work. The explanation for this difference in behavior is not evident.

A certain amount of impurities in the form of Li<sub>2</sub>O, LiOH, LiOH·H<sub>2</sub>O and Li<sub>2</sub>CO<sub>3</sub> resulting from contact with the atmosphere existed in all the samples. Some purification of the films probably resulted by using the evaporation procedure to form the thin films since none of the above impurities evaporate; all decompose. However, the thin films probably became contaminated to some extent by atmospheric gases remaining in the vacuum chamber or admitted to the interior of the cell through small leaks. The extent to which impurities affect the spectra is not known. In fact, little is known about the effect of impurities on transmission spectra, although some theoretical work has been done in connection with linear chains which indicates that the presence of impurities leads to a broad absorption on the high wavelength side of the main absorption peak. Consequently, the presence of impurities may account, in part, for the broad absorption band obtained above 17µ with Li<sup>6</sup>H<sup>1</sup> and Li<sup>7</sup>H<sup>1</sup>.

## A. Effect of Isotopic Mass: Li<sup>6</sup>H<sup>1</sup>, Li<sup>6</sup>H<sup>2</sup>, Li<sup>7</sup>H<sup>1</sup>, Li<sup>7</sup>H<sup>2</sup>.

For the relatively pure samples of (Li<sup>6</sup>;H<sup>1</sup>, H<sup>2</sup>) and (Li<sup>7</sup>;H<sup>1</sup>, H<sup>2</sup>), it was found (see Table II) that the ratio of the dispersion wavelengths for the various samples was in excellent agreement with the prediction of the elementary portions of the Born theory, namely, that this ratio should be the same as that of the square root of the reduced masses, if the mixture of the lithium or hydrogen isotopes can be considered as equivalent to a single species of the average isotopic mass. A similar result had been indicated in the findings of Montgomery and Misho<sup>13</sup> with lithium-6 and lithium-7 fluoride, but the present results are more definitive in view of the large relative difference in mass of the hydrogen isotopes (67%) in comparison with the lithium isotopes (15%).

The observed value of 17.0 $\mu$  for the dispersion wavelength of thin films of lithium-7 hydride agrees quite well with the estimate of 16.7 $\mu$  by

Filler and Burstein<sup>14</sup> from their data on the infrared reflectivity of thick crystals of lithium hydride.

That the elementary Born theory works well (at least to a first approximation) for a surprisingly large number of crystals has been shown by others<sup>3, 15</sup> by comparing the theoretical predictions with observed values for such quantities as the high-frequency dielectric constant, and compressibility. The present agreement between theory and experiment in the case of the variation of the infrared dispersion wavelength with isotopic mass constitutes another check on the validity of the simple Born theory.

### B. Effect of Isotopic Composition: Li<sup>6</sup>[xH<sup>1</sup>, (1-x)H<sup>2</sup>]

As indicated in Table IV, the observed variation of the infrared dispersion frequency with composition of a film made from an evaporated mixture of Li<sup>6</sup>H<sup>1</sup> and Li<sup>6</sup>H<sup>2</sup> disagrees markedly with the theoretical prediction of equation (21) when an average reduced mass for the molecules making up the composite film is simply used. In fact, the variation with composition does not appear to be simple in any way.

Although there is a 8 C<sup>o</sup> difference in the melting points of Li<sup>6</sup>H<sup>1</sup> and Li<sup>6</sup>H<sup>2</sup>, and probably an even greater difference in their boiling points, observation showed that the two compounds evaporated at the same rate at the temperature during which evaporation was carried out. This observation consisted in making successive evaporations from a boat containing a sample of composition 19.9% Li<sup>6</sup>H<sup>1</sup> and 80.1% Li<sup>6</sup>H<sup>2</sup> until the sample was completely gone. After each evaporation a spectrum was obtained which was identical with the previous spectra within experimental error.

Therefore, the effect appears to be a property of the complex crystal lattice, and it cannot be explained simply by considering the

composite film as being equivalent to one made up of isotopes with the average reduced mass. As mentioned earlier, the theory of the effect of isotopic composition on the infrared absorption spectrum of an ionic crystal has not been developed to the point where it can be compared with experimental results.

### C. Measurement of Film Thickness

Measurements of the thickness of a lithium hydride film on a flat glass plate by using the multiple-beam interference method were accurate to about ± 50 angstroms or less. However, it is doubtful that these measurements give the true thickness of the film on the KBr substrate in the sample cell since the flat glass plate, which acted as a substrate for the lithium hydride film on which measurements were made, had to be placed to one side of the sample cell. Although the edge of the glass plate was located only about one inch from the KBr substrate, it is conceivable that this difference in location might appreciably affect the thickness of the film on the two substrates for the thin films used in this work. A change in thickness of about 0.01 µ could, in fact, be detected over a one inch length of a step crossed by the interference fringes. Therefore, the film thicknesses are listed on the graphs of Figures 11 and 12 to only the nearest  $0.01\mu$ . No attempt was made to improve these measurements since an order of magnitude for the film thickness was adequate for this work.

#### REFERENCES CITED

- 1. E. W. Montroll and R. B. Potts, Phys. Rev. 100, 525 (1955),
- 2. J. Pirenne, Physica 24, 73 (1958).
- 3. M. Born and K. Huang, <u>Dynamical Theory of Crystal Lattices</u> (Clarendon Press, Oxford, England, 1954), Chap. 2.
- 4. K. Huang, Proc. Roy. Soc. A, 208, 352 (1951).
- 5. H. Frohlich, Theory of Dielectrics (Clarendon Press, Oxford England, 1958), 2nd ed.
- 6. J. A. Stratton, Electromagnetic Theory (McGraw-Hill Book Company, Inc., New York, 1941), Chap. 9.
- 7. T. R. P. Gibb, Jr. and C. E. Messer, A. E. C. Report NYO-3957, May 2, 1954; A. E. C. Report NYO-8022, August 31, 1957.
- 8. O. S. Heavens, Optical Properties of Thin Solid Films (Butterworths Scientific Publications, London, England, 1955), Chap. 5.
- 9. S. Tolansky, Multiple-Beam Interferometry of Surfaces and Films (Clarendon Press, Oxford, England, 1948), Chaps. 5 and 12.
- 10. R. B. Barnes and M. Czerny, Zeit. f. Phys. 72, 447 (1931).
- 11. R. F. Wallis and A. A. Maradudin, Bull. Am. Phys. Soc. II, <u>5</u>, 198 (1960).
- 12. Handbook of Chemistry and Physics (Chemical Rubber Publishing Co., Cleveland, Ohio, 1955), pp. 536-539.
- 13. D. J. Montgomery and R. H. Misho, Nature 183, 103 (1959).
- 14. A. S. Filler and E. Burstein, Bull. Am. Phys. Soc. II, 5, 198 (1960).
- K. Højendahl, K. Danske Vidensk. Selskab 16, No. 2 (1938);
   W. Shockley, Phys. Rev. 70, 105(A) (1946); B. Szigeti, Proc. Roy. Soc. A, 204, 51 (1950).

# PHYSICS-MATH LIB;

May live

JAN 1 3 165

JAN 28'6#

JUL 8 1370

MICHIGAN STATE UNIV. LIBRARIES
31293017430046